Task activation of the human brain studied in real time by functional magnetic resonance imaging

N. R. Jagannathan* and P. Raghunathan

Department of Nuclear Magnetic Resonance, All India Institute of Medical Sciences, Ansari Nagar, New Delhi 110 029, India

This paper describes our initial results on functional brain mapping using a whole-body clinical magnetic resonance (MR) scanner operating at 1.5 T and having no echo planar imaging capability. The focus is on the effects of motor cortex stimulation of normal volunteers using a circularly polarized head coil when a gradient echo pulse sequence is employed. The study demonstrates the technical feasibility of functional MR imaging by using conventional gradient echo sequence and equipment.

MAGNETIC resonance imaging (MRI) is a well-established noninvasive clinical diagnostic tool which produces a spatial display of hydrogens present in the human body and provides a high-resolution morphological picture of the anatomy with superior contrast resolution[1]. Recent developments in MRI methodology have demonstrated the possibility of observing human brain function[2–15]. 'Functional' imaging (fMRI) has great potential for assessing individual pathophysiology and for characterization of human brain functions such as language, learning, memory, task activation, etc.[16]. Using the echo planar imaging (EPI) technique, Belliveau *et al.*[2] described the measurement of blood volume during visual activation, which not only opened up exciting new possibilities in the study of brain physiology but also provided a unique and challenging tool for neuroscience. Since then, several research groups have demonstrated that functional imaging of the human brain was feasible on their conventional MR system, where EPI capabilities were not available[6–15].

In this paper, we present our initial experimental results on task activation studies using the fMRI technique. Our studies have been carried out on normal volunteers using a Siemens MAGNETOM 63SP-4000 whole-body scanner. Our objective was to evaluate and demonstrate the feasibility of such studies on our 1.5 T whole-body scanner, using the FLASH sequence[17].

Experiments were performed on the 1.5 T superconducting whole-body scanner using a circularly polarized head coil. Magnetic field shimming with all first-order coils was performed by means of global shimming for each subject, achieving typical line widths of about 15 Hz. Scout images, one in each orthogonal plane, were initially obtained. Later, multislice T_1-weighted images in the sagittal, and in some cases coronal, planes were obtained using the standard spin echo sequence with an echo time (TE) of 15 ms, repetition time (TR) of 520 ms, a 256 × 256 matrix and a slice thickness of 5 mm. Using these images as an anatomic guide, appropriate tilted planes were then selected for task activation studies. One or more of the tilted axial planes passing through the primary motor and sensory cortex (Figure 1) were selected. The pulse sequence used was a conventional two-dimensional, refocused gradient echo FLASH sequence[17,18] with TR = 90 ms, TE = 60 ms, flip angle = 40°, matrix size 64 × 128, field of view (FOV) = 200 mm, and slice thickness = 8 mm.

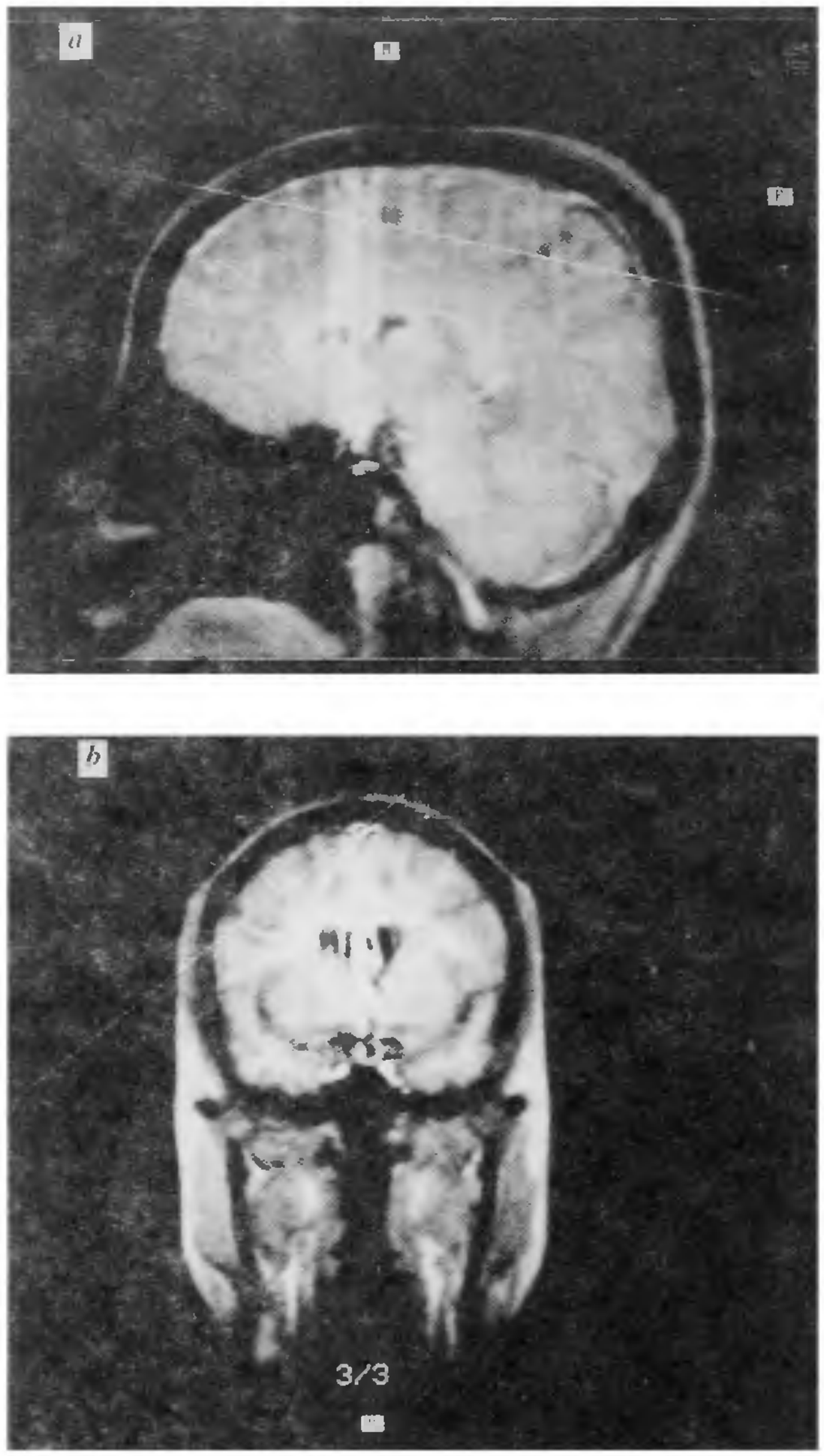

Figure 1. Proton MR images illustrating the orientation of the axial planes selected for task activation studies: *a*, for observing both the hemispheres of the brain simultaneously; *b*, for observing the left-hand movement on the right hemisphere of the brain.

*For correspondence.

These were optimized parameters, selected on the basis of a number of preliminary experiments. The percentage increase in signal intensity varies approximately linearly with TE; however, due to T_2^* processes, the overall signal intensity in both the control and activated images are known to decline with TE for a chosen tip angle of the RF pulse[9]. The maximum signal intensity increase in absolute terms occurs at a TE value approximately equal to T_2^*, which is around 66 ms in the activated region at 1.5 T (refs 6, 9). Our preliminary experiments also gave similar results and hence a TE value of 60 ms was used for all fMRI studies.

The hand task activation consisted of the volunteers ($n = 4$) either holding a sponge in the left or right hand and squeezing it repetitively, or performing finger-to-thumb movements. The rate and force of the squeezing of the sponge and finger-to-thumb movements were not controlled. Data were collected in blocks of 10 control images (i.e. in the task-free resting state), followed by 10 obtained during task activation (Figure 2). This procedure was repeated 4 or 5 times for each hand movement. When the axial plane shown in Figure 1 *a* was used, both left and right motor cortices were observed simultaneously. For this study, the volunteers ($n = 3$) held the sponges in both the hands and were asked to squeeze them simultaneously.

The MR images were reconstructed in the standard manner. Necessary postprocessing such as addition and subtraction of images was carried out using specialized software packages.

Figure 3 *a* shows an oblique T_1-weighted spin echo image of the anatomy of the selected section for subsequent monitoring of task activation, obtained using Figure 1 *b* as a pilot image. Figure 3 *b* shows the effects of left-hand movement; the appropriate cortical activity can be clearly seen near the sulcal wall. For observing both left and right motor cortices simultaneously, an axial oblique through a sagittal section was used as shown in Figure 1 *a*. Figure 3 *c* shows one such activated image when the volunteer was asked to activate both the hands, as described earlier. In general, the maximal signal intensity increase for the appropriate slice thickness used has been computed to be around 3–8%.

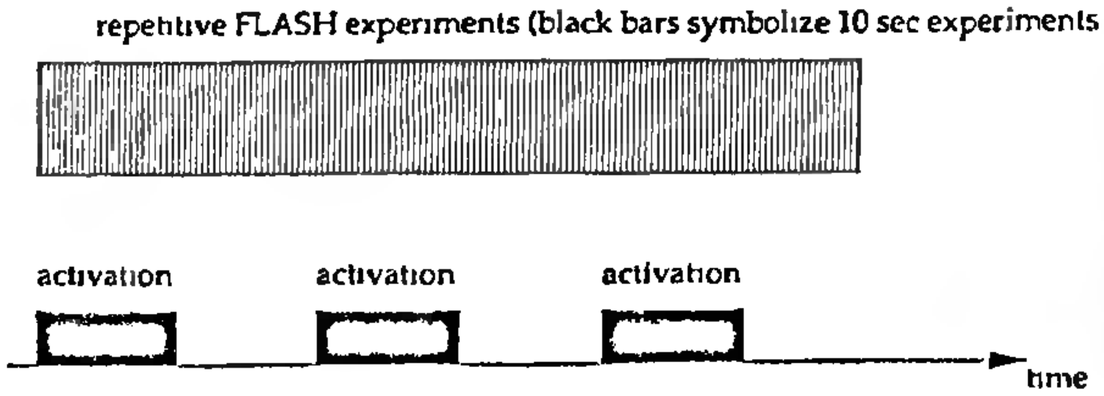

Figure 2. Experimental protocol for motor cortex activation. During 'activation' the volunteer performs the task of squeezing the sponge or finger-to-thumb motion

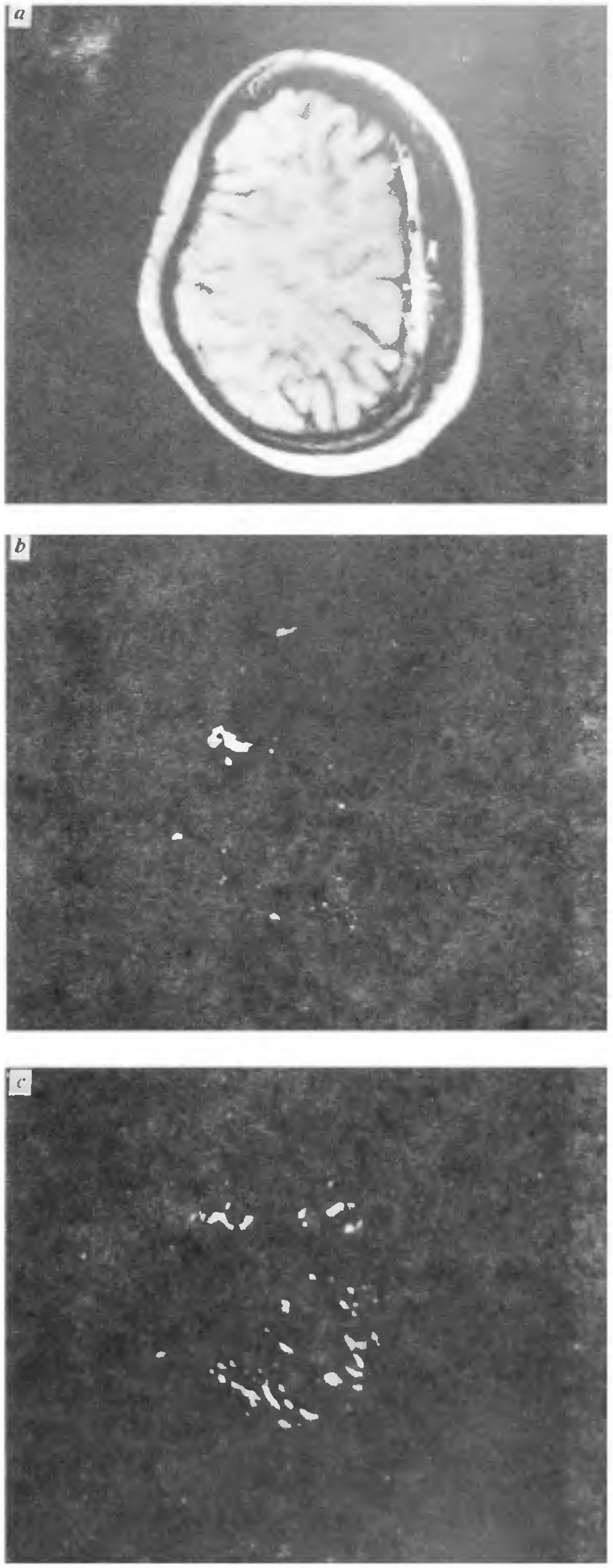

Figure 3. Images from a study of task activation obtained using the section orientation shown in Figure 1 *b*. *a*, Anatomy of the selected section. *b*, Effects of activation of the left hand task. *c*, Effects of activation during the task performed using both the hands simultaneously

The images shown in Figure 3 *c* are suitable for simultaneous examination of both left and right motor cortices. However, oblique planes through one hemisphere of the brain are preferable for viewing the detailed functional anatomy of the primary motor and sensory cortices. It is clear from Figures 3 *b* and *c* that activation is seen in grey matter of the sulcal walls, with little or no apparent effect in the intervening white matter[9]. In addition, the region activated by the hand movement task can also be precisely defined and related to specific gyri and sulci at a deeper level by following the activation down through successive sections using the three different planes shown in Figure 4 *a*. The set of images thus obtained from the right hemisphere of the brain from the superficial and middle planes are shown in Figures 4 *b* and *c* for the left-hand movement (see figure caption for details). As is seen clearly, the activation manifests itself as a hyperintense patch in the grey matter on both walls of the central sulcus. Other minor signal enhancement regions are also observed, showing that the area of activation is not confined to the walls and to the central sulcal region. These enhancement regions are believed to be associated with venous microvasculature in the grey matter[3].

The activation experiments were performed by first acquiring a set of 10 'activated' images – series A (during activation) – followed by 10 corresponding control rest images – series B (without any hand movement). This procedure of 'activity' (series A) followed by 'rest' (series B) was repeated 3 or 4 times. The image processing algorithm consists of adding together all the images of set A and producing a composite 'ACTIVE' image A. Then all images of series B, corresponding to rest period (no activation), were added together to produce a composite 'REST' image B. Finally, the algorithm takes the difference (A–B), and displays it as the 'functional MRI' image C. In this manner, the activation images shown in Figures 3 and 4 are the difference images obtained after 3 or 4 cycles of rest and activity. The accumulation of each data set takes about 800 s. The increase in signal intensity varied between 3 and 8%, depending upon the slice thickness used. However, the percentage signal intensity change depends on a number of factors such as partial volume effects, T_2^*, and other parameters used, such as the echo time, repetition time, slice thickness and, of course, the field strength. Intensity variations have also been known to occur if the postprocessing procedure is not correct. Subject movement during activation experiments may correlate with the task being performed and signal changes noticed may then be mistaken for evidence of brain activation[13]. Recently, several reports have appeared in the literature on these aspects and methods have been suggested to overcome these[19,20].

In our work, proper care has been taken regarding

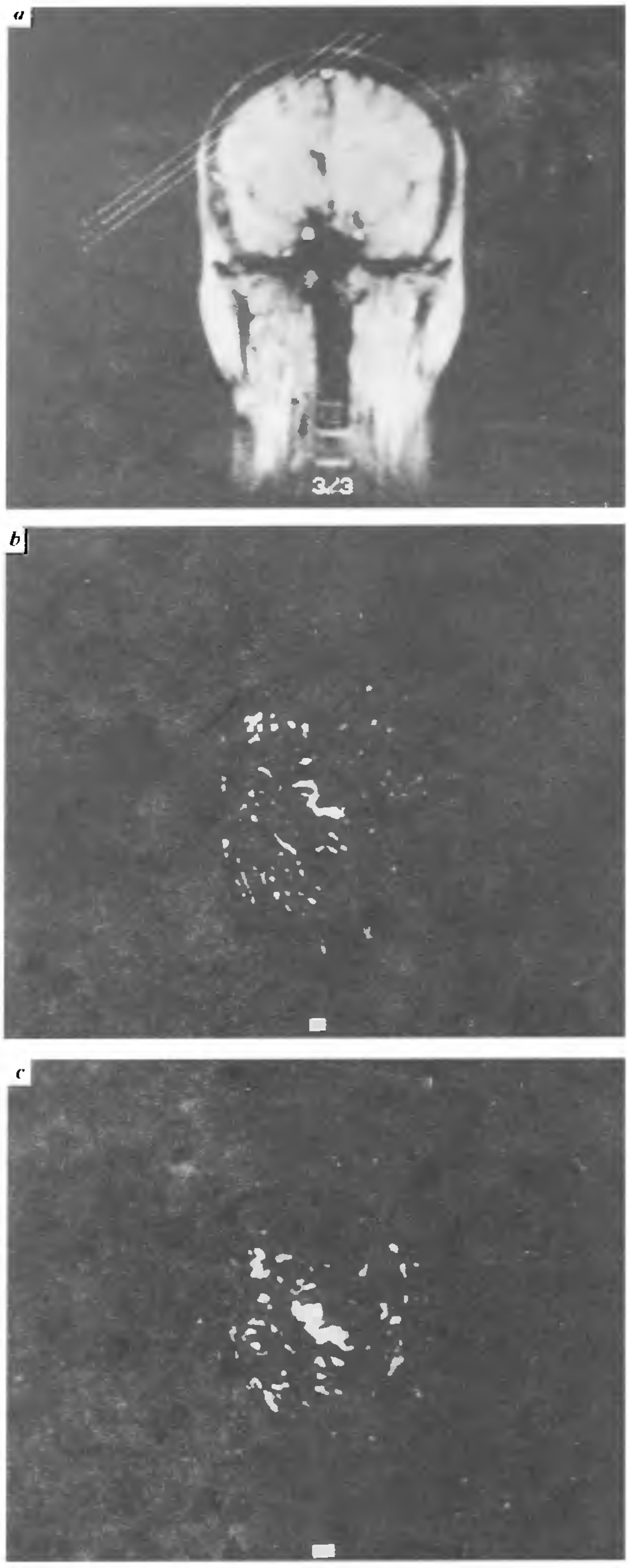

Figure 4. Images from a study of motor stimulation during left-hand movement task *a*, The different contiguous planes selected, superficial, middle and deep *b*, Activation in the superficial plane. *c*, Image from the middle plane. (The deep plane contains no image enhancement, denoting that it was not activated in hand movement and hence is not shown.)

subject movement during data acquisition to reduce motional artefacts. In addition, a set of 10 control (rest) images (with no activation – called set X) followed by another set of 10 control (rest) images (set Y) were separately acquired. All the images of set X were added together, producing a net 'REST' image X; similarly, all the images of set Y were added to produce another composite 'REST' image Y. The difference image, i.e. X–Y, was then obtained, which showed no signal enhancement in the plane selected, thus justifying that artefactual effects had been kept down to a minimum in executing our postprocessing algorithm.

The increase in local signal intensity observed in Figures 3 and 4 may be explained on the basis of our understanding of the blood-oxygenation-level-dependent (BOLD) mechanism whereby changes in neuronal activity affect the MR signal[21,22]. During task activation, brain stimulation takes place with increased blood flow, and oxygen delivery to the activated region exceeds the metabolic need[23]. The rise in blood supply seems to exceed the rise in oxygen consumption, leading to a local decrease in the ratio of deoxyhaemoglobin to oxyhaemoglobin[21,22]. Deoxyhaemoglobin is a paramagnetic substance and acts as an effective endogenous contrast agent. Moreover, a decrease in deoxyhaemoglobin concentration also decreases the vessel tissue susceptibility differential (leads to increased T_2^*), allowing increased spin coherence and thus increased signal while using a gradient echo sequence such as FLASH.

The functional MR images presented in this paper demonstrate that it is possible to use a conventional 1.5 T MR imager without echo planar capability for monitoring the brain functions if a gradient echo pulse sequence such as FLASH is employed. The application potential of fMRI is enormous in the area of neurosciences for assessing individual pathophysiology and for characterization of several brain functions[16] related to language[24], memory etc. In addition, it may also have important applications in neurosurgery. Identification of the anatomical relationship of a functional area to a tumour (which often distorts and displaces normal anatomy) is a great help to the neurosurgeon while planning the surgical approach and to preserve these primary areas during therapeutic operations[9].

1. Stark, D. and Bradley, W. (eds), *Magnetic Resonance Imaging*, Mosby, St. Louis, MO, 1992, 2nd edn.
2. Belliveau, J W., Kennedy, D. N., Mckinstry, R. C., Buchbinder, B. R, Weisskoff, R. M., Cohen, M. S, Vevea, J. M., Brady, T. J. and Rosen, B R., *Science*, 1991, **254**, 716–719.
3. Ogawa, S., Tank, D. W., Menon, R. S., Ellermann, J. M, Kim, S. G, Merkle, H and Ugurbil, K., *Proc. Natl Acad. Sci. USA*, 1992, **89**, 5951–5955.
4. Bandettini, P. A., Wong, E. C., Hinks, R. S., Tikofsky, R. S. and Hyde, J. S, *Magn. Reson. Med.*, 1992, **25**, 390–397.
5. Turner, R, Jezzard, P., Wen, H., Kwong, K. K, LeBihan, D., Zeffio, T. and Balaban, R., *Magn. Reson. Med.*, 1993, **29**, 277–279.
6 Balmire, A. M, Ogawa, S., Ugurbil, K., Rothman, D, McCarthy, G., Ellerman, J. M., Hyder, F., Rattner, Z. and Shulman, R. G., *Proc. Natl. Acad. Sci USA*, 1992, **89**, 11069–11073.
7. Frahm, J., Bruhn, H., Merboldt, K. and Hanicke, W., *J. Magn. Reson. Imaging*, 1992, **2**, 501–505.
8 Frahm, J., Merboldt, K and Hanicke, W., *Magn. Reson. Med.*, 1993, **29**, 139–144.
9. Connelly, A., Jackson, G. D., Fracknowiak, R. S. J., Belliveau, J. W., Vargha-Khadem, F. and Gadian, D. G., *Radiology*, 1993, **188**, 125–130.
10. Kim, S. G, Ashe, J., Hendrich, K., Ellermann, J. M., Merkle, H., Ugurbil, K. and Georgopoulos, A. P., *Science*, 1993, **261**, 615–617.
11. Schneider, W., Noll, D. C. and Cohen, J. D., *Nature*, 1993, **365**, 150–153.
12. Duyn, J. H., Moonen, C. T. W., deBoer, R. W., vanYperen, G. H. and Luyten, P. R., *NMR Biomed.* 1994, **7**, 83–88.
13. Constable, R. T., McCarthy, G., Allison, T., Anderson, A. W. and Gore, J. C., *Magn. Reson. Imaging*, 1993, **11**, 451–459.
14. Schad, L. R, Trost, U., Knopp, M V, Muller, E. and Lorenz, W. J., *Magn. Reson. Imaging*, 1993, **11**, 461–464.
15. Constable, R. T., Kennan, R. P., Puce, A., McCarthy, G. and Gore, J. C., *Magn. Reson. Med.*, 1994, **31**, 686–690.
16 Rosen, B R., Belliveau, J. W., Aronen, H J., Hamberg, L. M., Kwong, K. K. and Fordham, J. A., in *Magnetic Resonance Neuroimaging* (eds Kucharczyk, J., Moselay, M. and Barkovich, A J.), CRC Press, Boca Raton, 1994, pp. 141–166.
17. Hasse, A., Frahm, J, Marthaei, D., Hanicke, W. and Merboldt, K D., *J. Magn. Reson*, 1986, **67**, 258–266.
18. Hasse, A, Frahm, J, Matthaei, D., Merboldt, K. D. and Hanicke, W., in *Book of Abstracts*: Fourth Annual Meeting of the Society of Magnetic Resonance in Medicine, SMRM, London, 1985, pp. 980–981.
19. Hajnal, J V., Myers, R, Oatridge, A., Schwieso, J. E., Young, I. R. and Bydder, G. M., *Magn. Reson Med.*, 1994, **31**, 283–291.
20. Hu, X. and Kim, S. G., *Magn. Reson. Med.*, 1994, **31**, 495–503.
21. Ogawa, S., Lee, T. M., Kay, A. and Tank, D., *Proc. Natl. Acad. Sci USA*, 1990, **87**, 9868–9872.
22 Ogawa, S., Lee, T. M., Nayak, A. S. and Glynn, P., *Magn. Reson. Med.*, 1990, **14**, 68–78.
23. Fox, P. T. and Raichle, M. E., *Proc. Natl. Acad. Sci. USA*, 1986, **83**, 1140–1144.
24. Shaywitz, B A., Shaywitz, S. E., Pugh, K. R, Constable, R. T., Skudlarski, P., Fulbright, R. K., Bronen, R. A., Fletcher, J. M., Shankweiler, D. P., Katz, L. and Gore, J. C., *Nature*, 1995, **373**, 607–609.

ACKNOWLEDGEMENTS We thank Profs P. N. Tandon and A. K. Banerji for their interest, encouragement and critical evaluation of the manuscript, Dr V. Govindaraju for many useful discussions and Dr R. Jayasundar for making available the processing software from Erlangen. Financial support from the Department of Science and Technology and Department of Biotechnology in the initial acquisition of MRI equipment is gratefully acknowledged.

Received 20 May 1995, revised accepted 10 July 1995